

Original citation:

De-Giovanni, Mario, Alam, Talukder, Banerjee, Rajarshi and Srirangam , Prakash (2018) *3D atom probe tomography study on segregation of yttrium in modified Al-Si alloys*. JOM . doi:[10.1007/s11837-018-2909-x](https://doi.org/10.1007/s11837-018-2909-x)

Permanent WRAP URL:

<http://wrap.warwick.ac.uk/102372/>

Copyright and reuse:

The Warwick Research Archive Portal (WRAP) makes this work of researchers of the University of Warwick available open access under the following conditions.

This article is made available under the Creative Commons Attribution 4.0 International license (CC BY 4.0) and may be reused according to the conditions of the license. For more details see: <http://creativecommons.org/licenses/by/4.0/>

A note on versions:

The version presented in WRAP is the published version, or, version of record, and may be cited as it appears here.

For more information, please contact the WRAP Team at: wrap@warwick.ac.uk

3D Atom Probe Tomography Study on Segregation of Yttrium in Modified Al-Si Alloys

MARIO DE-GIOVANNI,¹ TALUKDER ALAM,² RAJARSHI BANERJEE,²
and PRAKASH SRIRANGAM^{1,3}

1.—WMG, University of Warwick, Coventry CV4 7AL, UK. 2.—Department of Materials Science and Engineering, University of North Texas, Denton 76203, USA. 3.—e-mail: p.srirangam@warwick.ac.uk

Yttrium segregation behavior in Al-Si alloys has been studied using the three-dimensional atom probe tomography technique. Al-Si alloys were prepared by casting method, and yttrium was added to modify the eutectic silicon morphology in these alloys. The results indicated that yttrium is preferentially located within the Si phase, with the highest concentration at the interface between eutectic Al and eutectic Si.

INTRODUCTION

Aluminum-silicon (Al-Si) alloys are widely used in automotive and aerospace industries due to their high strength-to-weight ratio, good castability, and excellent mechanical and performance properties.¹ The microstructure of eutectic and hypoeutectic Al-Si is very coarse, with the eutectic being made up of large platelets or needles of silicon in a continuous aluminum matrix. Alloys exhibiting this microstructure show poor ductility due to the large and brittle silicon plates. The ductility and tensile strength of these alloys can be improved by addition of modifying elements such as sodium, strontium, and rare-earth elements, which modify the eutectic silicon morphology from flake to fibrous shape.^{1–3} The change in size and shape of the Si phase also improves the wear resistance of Al-Si alloys.⁴ Among all these modifying elements, Sr is considered to be the best for modifying Al-Si alloys. There has been an ongoing debate regarding the mechanism of modification of Al-Si alloys. In an attempt to understand the modification mechanism, a number of researchers have looked into the segregation behavior of modifying elements within the alloy. Clapham and Smith,⁵ used atomic absorption spectroscopy (AAS) and observed that Sr is preferentially located in the Si phase. Nogita et al.⁶ used synchrotron-based micro-x-ray fluorescence (μ XRF) and noted that Sr was segregated within the eutectic Si phase. Atom probe tomography (APT) has been used by several researchers to look into the segregation of the modifying element within Al-Si alloys.^{7–12} Past studies have explored the

application of Y as a modifier of Al-Si alloys. Researchers used varying amounts of Y, between 200 ppm and 6000 ppm, and observed that, in presence of Y, the Si eutectic forms a refined plate-like morphology rather than a fibrous one.^{13–15} However, no studies have reported on the segregation behavior of yttrium in such modified Al-Si alloys. In the work presented herein, for the first time, the segregation behavior of yttrium in Al-Si alloy was studied using atom probe tomography; the results obtained from this study are presented and discussed.

METHODOLOGY

Alloy Preparation

Al-Si alloy was prepared by melting 99.999% purity aluminum (NewMet, UK) in a clay graphite crucible using a Carbolite RHF1500 high-temperature chamber furnace. Silicon (99.999%, Alfa Aesar, UK) was added to the molten aluminum and stirred in. Once melting was complete, the mixture was poured into a preheated clay graphite crucible and left to solidify. Al-Si was then used to prepare Al-Si-Y alloy. The Al-Si alloy was molten, then Al-10Y (wt.%) master alloy was added employing the same procedure. This master alloy was produced using a similar procedure using the same 99.999% purity aluminum and 99.9% purity yttrium (Alfa Aesar, UK). The chemical compositions of the two alloys were analyzed by inductively coupled plasma optical emission spectroscopy (ICP-OES) and are presented in Table I.

Table I. Chemical composition of Al-Si and Al-Si-Y in weight percentage

	<u>Al</u>	<u>Si</u>	<u>Y</u>	<u>Fe</u>	<u>Cu</u>	<u>Mn</u>
Al-Si	Balance	8.82	–	< 0.01	< 0.01	< 0.01
Al-Si-Y	Balance	7.75	1.09	< 0.01	< 0.01	< 0.01

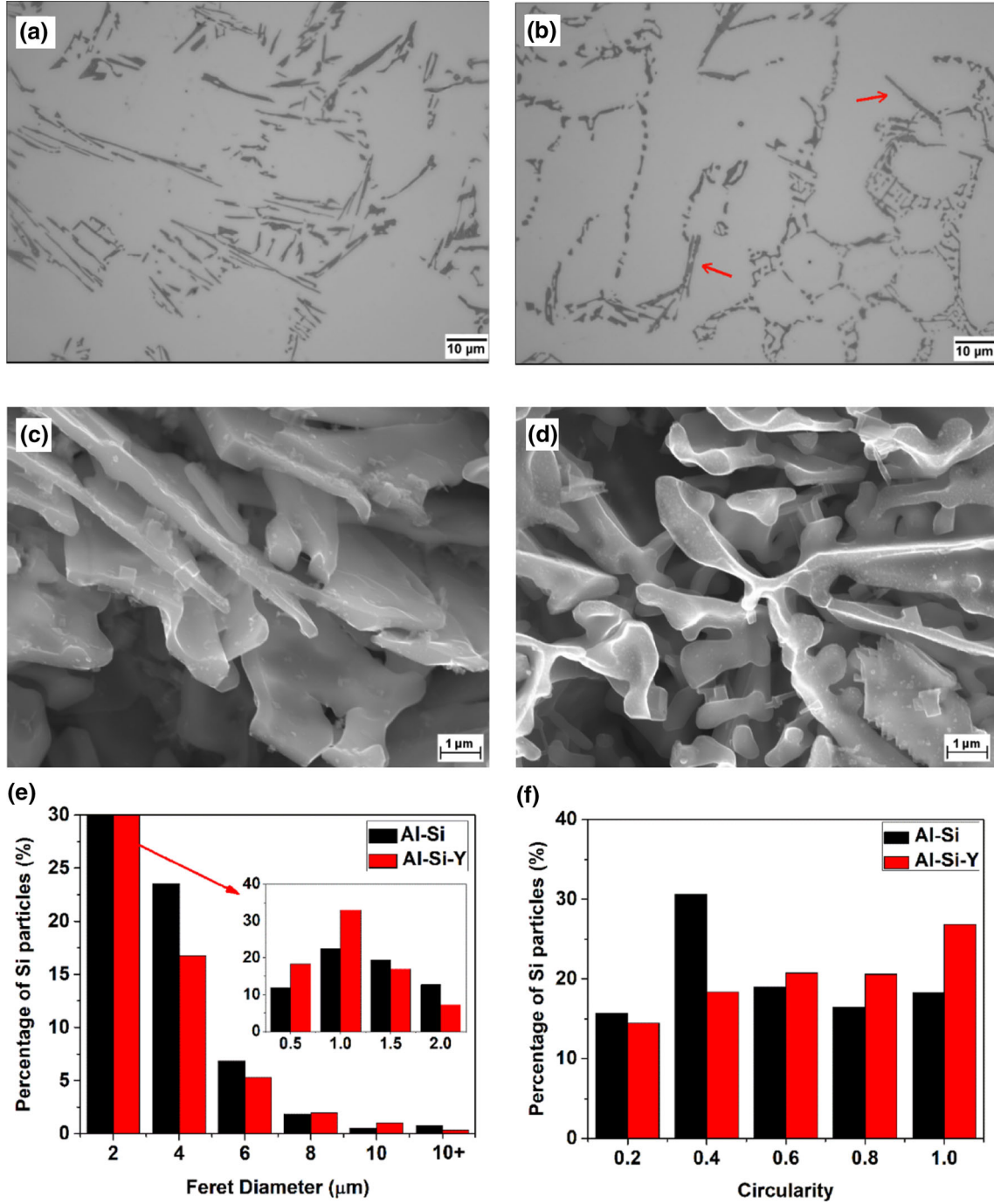


Fig. 1. Optical micrographs showing (a) unmodified Al-Si alloy and (b) modified Al-Si-Y alloy. SEM images of etched samples of (c) unmodified Al-Si alloy and (d) modified Al-Si-Y. (e) Size and (f) shape analysis of Si phase extracted from SEM images at $\times 5k$.

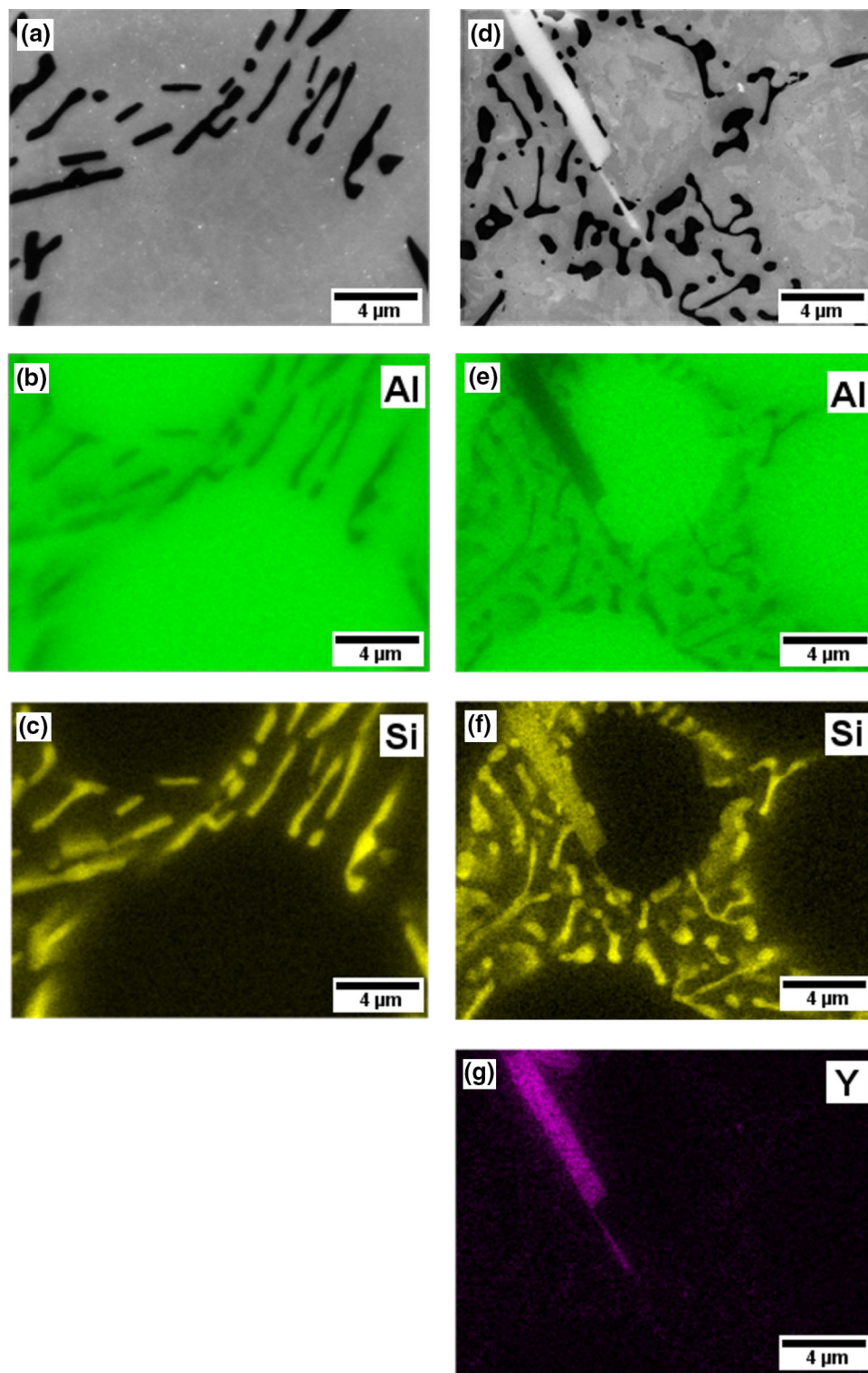


Fig. 2. SEM images representing (a) unmodified Al-Si and (d) Al-Si-Y alloy, and EDS maps representing elemental analysis for corresponding Al (b, e), Si (c, f), and Y (g) (color figure available online).

Microstructural Analysis

Metallographic samples were prepared from cast cylinders for microstructural analysis by optical microscopy and scanning electron microscopy

(SEM). Chemical analysis was performed by energy-dispersive spectroscopy (EDS). Etching was performed using 20% hydrochloric acid (37%) and 80% isopropyl alcohol mixture, to reveal the fibrous

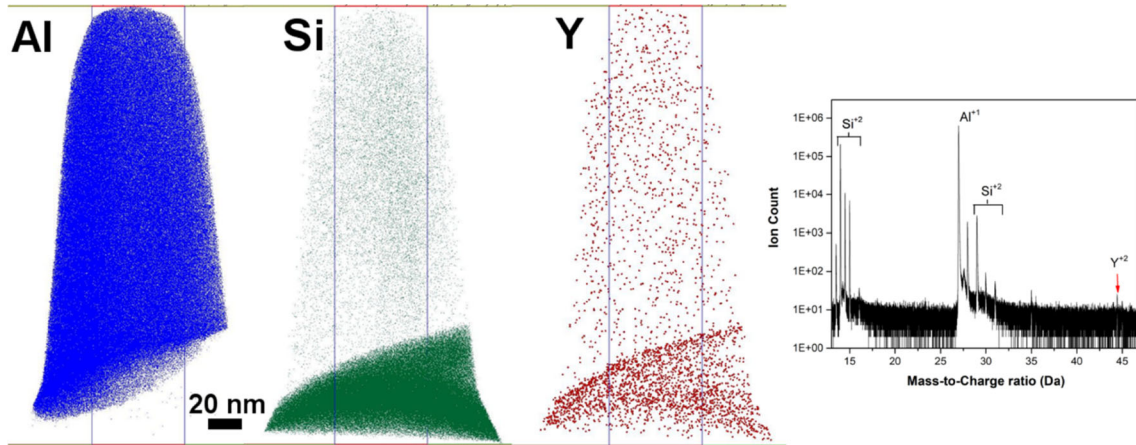


Fig. 3. Raw ion maps of the whole APT reconstruction of Al-Si alloys modified with yttrium, including the mass-to-charge ratio spectra with identified Al, Si, and Y peaks (color figure available online).

or lamellar structure of the Si eutectic. Five SEM images per composition were acquired at $5000\times$ magnification and analyzed by using thresholding in ImageJ software.

Atom Probe Tomography

Site-specific APT specimens were prepared in a dual-beam focused ion beam (FIB)/SEM (FEI Nova 200 NanoLab) by standard lift-out method utilizing Pt deposition and a micromanipulator. A long bar was detached from the surface using the micromanipulator and transferred to prefabricated Si posts on a coupon, and small cut sections ($\sim 2\text{ }\mu\text{m}$ long) of the bar were welded on the Si posts. A procedure similar to that carried out in this research was described by Felfer et al.¹⁶

The samples mounted on the Si posts were annular milled to prepare taper-shaped needles with end radius of 20 nm to 40 nm. Under high vacuum and low temperature of 40 K, ions from the surface of this needle were evaporated inside the LEAP (Cameca 3000X HR). The energy for evaporation was supplied by a 512-nm green laser with laser pulse energy of 0.5 nJ. An automatic evaporation control protocol was employed to maintain steady-state evaporation of 0.5%. Raw APT data were collected from the LEAP, and reconstructed using the IVAS[®] 3.6.10 software package.

RESULTS

Figure 1a and b shows optical images of the unmodified and Y-modified Al-Si alloys. From these images, it is clearly visible that Si eutectic is present in the form of plate-like structures in the unmodified alloy, whereas in the Y-modified alloy, the Si phase is present as finer lamellar structures. These structures are shown in greater detail in the images of etched samples in Fig. 1c and d. In the optical microscopy images, one can also observe the presence of a ternary phase in the Y-modified alloy. The

arrows indicate two ternary-phase particles, however identifying these ternary phases is difficult due to similar contrast to the Si phase. The modification effect of yttrium was analyzed quantitatively, in terms of Feret diameter and circularity, by analyzing a number of SEM images. It must be clarified that the quantitative analysis was performed on a two-dimensional (2D) cross-section and thus yields information regarding the apparent size and shape of the Si eutectic in this plane. The Feret diameter is defined as the longest distance between any two points along the selection boundary.¹⁷ Circularity is defined by $4\pi \times \frac{\text{Area}}{\text{Perimeter}^2}$, where a value of 1 indicates a perfect circle, with decreasing values indicating a less circular feature.¹⁷ Histograms are presented in Fig. 1e and f, showing that the Feret diameter in the samples containing Y was typically smaller. A further indication of the marginal modification after Y addition is given by the higher circularity of the Si phase in this alloy.

Figure 2 presents SEM images, including chemical analysis. The electron images yield similar information to the optical microscopy images, though at higher magnification. Furthermore, the ternary-phase intermetallics have bright contrast. The chemical analysis images show that Y was found mainly in the ternary intermetallic phase. The concentration of Y in eutectic Si or primary Al would be very low, hence detection of such small concentrations by means of EDS would be difficult and unreliable. Similar ternary intermetallic precipitates were observed at concentrations as low as 200 ppm Y.¹⁵

Figure 3 shows raw ion maps of the whole reconstructed area. From this map it can be observed that there is a clear distinction between the Al and Si phases, and the presence of the different elements in the other phases is minimal. From these raw ion maps, it can also be observed that, although Y is present throughout the entire sample, it is preferentially located in the Si phase.

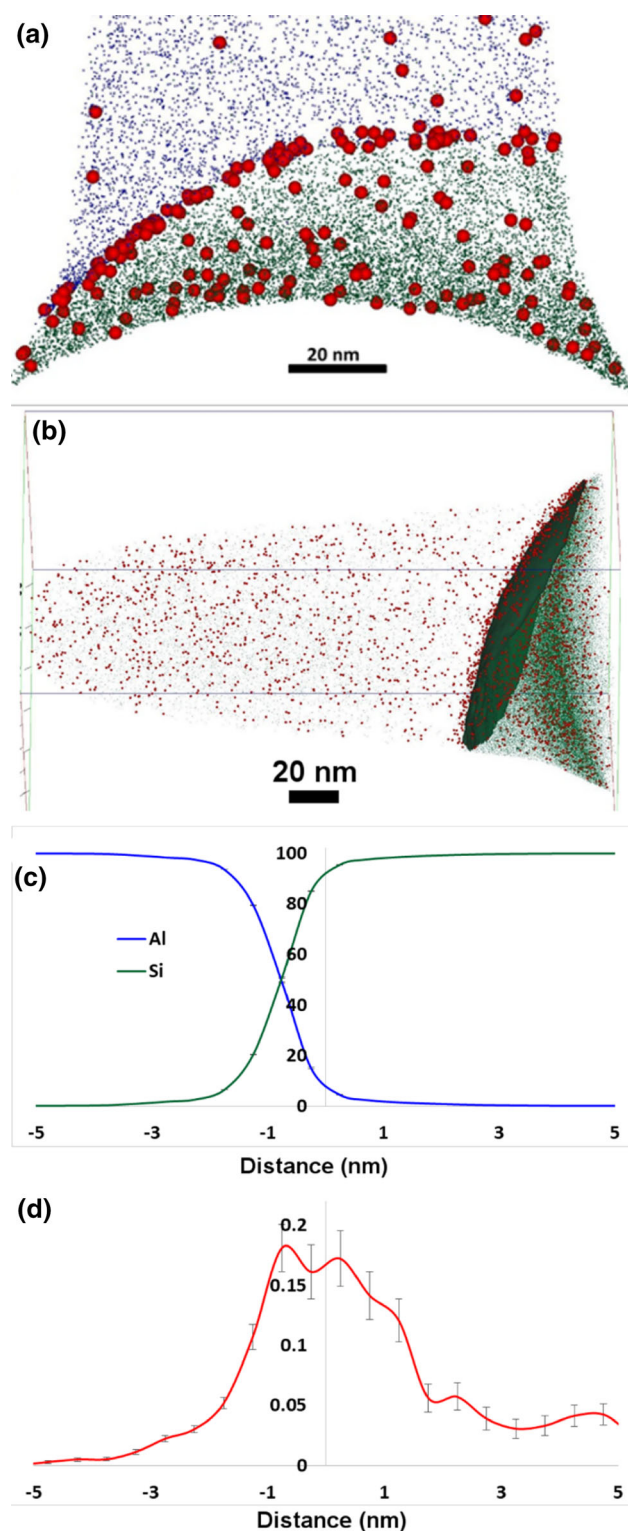


Fig. 4. (a) 15-nm slice view of reconstruction showing segregation of Y in the phase boundary. Y ions (red spheres) are clearly seen at the interface of Al-rich and Si-rich phase. (b) Isoconcentration surface of Si at 50% outlines the phase boundary between the Al-rich and Si-rich phases. (c) Proxigram generated from the isosurface reveals the Al and Si partitioning between the phases. (d) Proxigram of Y clearly reveals that it is segregated in the phase boundary and preferentially partitions to the Si-rich phase (color figure available online).

Figure 4a shows a 150-nm cropped section across the phase boundary between the Al and Si phases. The Y ions, depicted as red spheres, are clearly seen to segregate at the Si phase, with higher presence at the phase boundary. This segregation at the boundary could occur due to Y atoms being pushed out of the solidifying phases, thus a boundary that is rich in Y forms in this position.

Figure 4b and d shows the isoconcentration surface of Si = 50 at.%, outlining the phase boundary between the Al-rich and Si-rich phases with the corresponding proxigrams for Al, Si, and Y. From these, it can be observed that there is minimal mixing between the Al and Si phases. More importantly, Y is clearly revealed to be segregated at the phase boundary of the two phases and preferentially partitions into the Si-rich phase.

DISCUSSION

From the APT results obtained, it is clear that Y, similarly to other elements which fully modify the eutectic Si phase such as Sr and Na, segregates preferentially into the Si phase. Furthermore, Y seems to be pushed to the eutectic Si boundary. This behavior correlates with the findings of Li et al.¹¹ for Na modification but is in contrast to those of Srirangam et al.⁷ for Sr modification. Srirangam et al.⁷ noted segregation of Sr within the eutectic Si phase with no indication of enrichment at the interface, whereas Li et al.¹¹ noted Na enrichment at the interface between eutectic Si and eutectic Al in Na-modified Al-Si alloys. It is therefore indicative that the phase where the additional element segregates does not necessarily indicate the modification potential of the element.

Other authors have delved deeper into the eutectic Si and explored the characteristics of the Sr segregations within this phase. Timpel et al.^{8,9} noted that Sr is heterogeneously cosegregated with Al within the Si phase, and these form either a nanometer-scale rod-like segregation or more extended structures. The rod-like formations were regarded as being responsible for the twin formation and the enablement of growth in different crystallographic orientations, whereas the extended structures were believed to be responsible for growth restriction and branching of the Si crystal. The ability of these three elements to cosegregate was regarded as indicative that these promote formation of new twins. Barrirero et al.¹⁰ similarly identified rod-like nanoscale cosegregations (responsible for smoothening of Al-Si boundaries in eutectic phase) and particle-like and planar cosegregations (favoring formation of twin boundaries). The particle-like segregations were also observed in the unmodified alloy, though obviously containing exclusively Al. The authors further noted that the concentration of Al within the eutectic was approximately four times higher in the modified alloy when compared with the unmodified material, which further supports the

hypothesis that Al and Sr are incorporated together into the Si phase in the form of nanometer-sized phases. Li et al.¹¹ investigated the segregation of sodium (Na), another well-known modifier, in Al-5Si alloy. They noted that similar rod-like and particle-like structures formed. Barriero et al.¹² also performed compositional analysis of the nanometer-sized clusters by means of APT, which indicated presence of NaAlSi and SrAl₂Si₂ in Na- and Sr-modified Al-Si alloys, respectively. They proposed that the clusters form at the Si/liquid interface and take part in the modification process by altering the eutectic growth. They suggest that the efficiency of a modifier depends on the ability to form ternary compound clusters at the Si/liquid interface near the binary eutectic point. Further research is required to investigate the segregation of Y within Si to identify whether Y within the Si phase is cosegregated with Al, similarly to the cases of Sr and Na, and the morphology of such segregations. Future studies involving extensive transmission electron microscopy (TEM) work is required to understand the effect of yttrium on formation of nano ternary compounds and twins in eutectic silicon phase in Al-Si alloys. However, the present study clearly shows that yttrium addition does not result in significant modification of the eutectic silicon morphology, although yttrium is found to be preferentially segregated in the silicon phase.

CONCLUSIONS

- Al-Si alloys are partially modified with addition of yttrium using casting method.
- Segregation behavior of yttrium was studied using 3D atom probe tomography.
- APT results clearly show that yttrium preferentially segregated in eutectic silicon phase and resulted in only partial modification of eutectic silicon.

OPEN ACCESS

This article is distributed under the terms of the Creative Commons Attribution 4.0 International Li-

cense (<http://creativecommons.org/licenses/by/4.0/>), which permits unrestricted use, distribution, and reproduction in any medium, provided you give appropriate credit to the original author(s) and the source, provide a link to the Creative Commons license, and indicate if changes were made.

REFERENCES

1. I.J. Polmear, *Light Alloy* (Amsterdam: Elsevier, 2005), pp. 205–235.
2. R. Bartley, *British and European Aluminium Casting Alloys* (Birmingham: Association of Light Alloy Refiners, 1996).
3. J.E. Hatch, *Aluminium: Properties and Physical Metallurgy*, 2nd ed. (Russell Township: American Society of Metals, 1984).
4. S.-L. Lee, Y.-C. Cheng, W.-C. Chen, C.-K. Lee, and A.-H. Tan, *Mater. Chem. Phys.* 135, 503 (2012).
5. L. Clapham and R.W. Smith, *J. Cryst. Growth* 92, 263 (1988).
6. K. Nogita, H. Yasuda, K. Yoshida, K. Uesugi, A. Takeuchi, Y. Suzuki, and A.K. Dahle, *Scr. Mater.* 55, 787 (2006).
7. P. Srirangam, S. Chattopadhyay, A. Bhattacharya, S. Nag, J. Kaduk, S. Shankar, R. Banerjee, and T. Shibata, *Acta Mater.* 65, 185 (2014).
8. M. Timpel, N. Wanderka, R. Schlesiger, T. Yamamoto, N. Lazarev, D. Isheim, G. Schmitz, S. Matsumura, and J. Banhart, *Acta Mater.* 60, 3920 (2012).
9. M. Timpel, N. Wanderka, R. Schlesiger, T. Yamamoto, D. Isheim, G. Schmitz, S. Matsumura, and J. Banhart, *Ultramicroscopy* 132, 216 (2013).
10. J. Barrirero, M. Engstler, N. Ghafoor, N. de Jonge, M. Odén, and F. Mücklich, *J. Alloys Compd.* 611, 410 (2014).
11. J.H. Li, J. Barrirero, M. Engstler, H. Aboulfadl, F. Mücklich, and P. Schumacher, *Metall. Mater. Trans. A* 46, 1300 (2015).
12. J. Barrirero, J. Li, M. Engstler, N. Ghafoor, P. Schumacher, M. Odén, and F. Mücklich, *Scr. Mater.* 117, 16 (2016).
13. A. Knuutinen, K. Nogita, S.D. McDonald, and A.K. Dahle, *J. Light Met.* 1, 229 (2001).
14. B. Li, H. Wang, J. Jie, and Z. Wei, *Mater. Des.* 32, 1617 (2011).
15. J.H. Li and P. Schumacher, *Int. J. Cast Met. Res.* 25, 347 (2012).
16. P.J. Felfer, T. Alam, S.P. Ringer, and J.M. Cairney, *Microsc. Res. Tech.* 75, 484 (2012).
17. W.R.T. Ferreira, *ImageJ User Guide IJ* 1, 46r (2012).